SAMoCo: A Learning-Initialized and Physics-Refined Framework for Sampling-Agnostic Motion Correction in MRI

Weijia Liu[1], Runyu Tang[1], Ye Yao[1], Yao Li[1], Hongming Shan[2], Hongjiang Wei[1], and Dengrong Jiang[1](✉)

[1] National Engineering Research Center of Advanced Magnetic Resonance Technologies for Diagnosis and Therapy, School of Biomedical Engineering, Shanghai Jiao Tong University, Shanghai, China

[2] Institute of Science and Technology for Brain-Inspired Intelligence, Fudan University, Shanghai, China

dengrongjiang@sjtu.edu.cn

Abstract. Patient motion during magnetic resonance imaging (MRI) acquisition leads to severe artifacts that degrade diagnostic quality. End-to-end deep learning (DL)-based motion correction methods are prone to structural hallucinations and often exhibit limited generalizability across different image contrasts. While some studies instead estimate motion parameters and perform model-based reconstruction to avoid hallucinations, they are typically restricted to specific k-space sampling patterns. To address these challenges, we present a novel retrospective motion correction framework that synergistically integrates DL-based motion estimation with model-based optimization and reconstruction. Our hybrid approach consists of two key components: (1) A pre-trained neural network that explicitly processes both undersampled k-space data and sampling patterns to infer motion parameters, enabling flexible adaption to variable numbers of shots and phase-encoding lines; specifically, this network combines convolutional neural network with gated recurrent unit, and is trained on a diverse simulated dataset encompassing varying image contrasts, anatomical orientations, and sampling patterns; (2) An instance-wise autofocusing algorithm that jointly refines the initial motion parameters and updates coil sensitivity maps, ultimately yielding artifact-free images. The proposed framework generalizes well across different image contrasts, k-space sampling patterns, and acceleration factors. Validations on fastMRI dataset and in-house MRI data demonstrate that our approach outperforms state-of-the-art methods in motion artifact suppression, while preserving strict physical fidelity and strong cross-protocol generalization capability. These results highlight the potential of our approach for robust clinical deployment.

Keywords: Motion correction · Autofocusing · Reconstruction · Sensitivity map estimation · Magnetic resonance imaging

1 Introduction

Magnetic resonance imaging (MRI) is a non-invasive imaging modality providing excellent soft-tissue contrast. However, patient motion during data acquisition remains a major challenge, often introducing structural artifacts that degrade image quality and compromise diagnostic reliability [5, 22]. Numerous retrospective motion correction methods have been developed to address this problem. Classical iterative reconstruction approaches based on autofocusing [4] or data-consistency [13] are physically grounded but often suffer from slow convergence and susceptibility to local minima [2]. With the rapid advancement of deep learning (DL), many learning-based approaches have been proposed to model the complex non-linear relationship between motion-corrupted images or k-space and their motion-free references [21, 23, 25]. However, end-to-end learning-based reconstruction remains prone to hallucinated structures and their performance frequently degrades when being applied to varying image contrasts [7].

To mitigate these issues, several studies have explored hybrid strategies that combine deep learning with model-based reconstruction. For instance, embedding a U-Net within the autofocusing framework effectively compensating for the limitations of each paradigm [18]. Other approaches pretrain networks to detect motion-corrupted k-space lines, which are then excluded or down-weighted in subsequent physics-driven reconstruction [8, 10]. However, their performance degrades when a large proportion of k-space is corrupted [2]. Another line of work estimates motion parameters directly from corrupted k-space, where the predicted parameters serve as reliable initializations or priors for subsequent physics-driven optimization [9, 14, 20, 24]. Despite these advances, the existing methods remain constrained by specific sampling trajectories. Moreover, these correction approaches assume coil sensitivity maps to be accurately known [15], which may not hold under motion-corrupted and undersampled acquisitions.

In this work, we propose a novel retrospective motion correction framework that integrates DL-based motion estimation with physics-driven optimization and reconstruction. The main contributions are threefold: (1) We trained a neural network that explicitly processes both undersampled k-space data and sampling patterns to provide reliable initial estimations of motion parameters; (2) We developed an instance-wise autofocusing algorithm and a model-based reconstruction framework to jointly refine motion parameters, estimate coil sensitivity maps, and reconstruct motion-corrected images; (3) We demonstrated the efficacy of our proposed method on fastMRI and in-house datasets, showing superior performance compared to state-of-the-art (SOTA) methods.

2 Methods

2.1 Physics Model and Problem Formulation

We focus on the retrospective motion correction problem in 2D multi-shot MRI, such as in common sequences like fast spin echo. We further assume that the subject undergoes rigid motion between shots and remains quasi-static during the readout of each shot [12]. Let $\mathbf{x} \in \mathbb{C}^N$ denote the ideal motion-free image. For a scan comprising N_s shots and N_c receiver coils, the motion-corrupted k-space measurement $\mathbf{y}_c$ for the c-th coil is modeled as follows:

$$\mathbf{y}_c = \sum_{j=1}^{N_s} \mathbf{M}^j \mathcal{F} \mathbf{S}_c \mathbf{T}^j \mathbf{R}^j \mathbf{x} \ , \tag{1}$$

where $\mathbf{M}^j$ represents the sampling mask for the j-th shot, $\mathcal{F}$ is the Fourier Transform, and $\mathbf{S}_c$ is the sensitivity map for the c-th coil. $\mathbf{T}^j$ and $\mathbf{R}^j$ denote the rotation and translation matrices, respectively, parameterized by the rotation angle θ^j and translation vector $\mathbf{t}^j = [t_x^j, t_y^j]^T$. Rigid rotation in the image domain is equivalent to a coordinate rotation in frequency domain [28]. For the j-th shot, the standard Cartesian frequency grid $\mathbf{k^j}$ is rotated to $\mathbf{k^j}'$:

$$\mathbf{k^j}' = \mathbf{R}(\theta^j)\mathbf{k} = \begin{bmatrix} \cos\theta^j & -\sin\theta^j \\ \sin\theta^j & \cos\theta^j \end{bmatrix} \mathbf{k} \ . \tag{2}$$

This transformation destroys the uniformity of the grid, necessitating a Non-Uniform Fast Fourier Transform (NUFFT) [11]:

$$\mathbf{y}_\theta = \mathrm{NUFFT}\{\mathbf{S}_c \mathbf{x}, \mathbf{k^j}'\} \ . \tag{3}$$

Subsequently, according to the Fourier shift theorem, the spatial translation $\mathbf{T}^j$ induces a linear phase shift in k-space. The final measured data for shot j is obtained by applying this phase modulation:

$$\mathbf{y}_{\theta,t} = \mathbf{y}_\theta \cdot \exp\left[-i2\pi(\mathbf{t^j} \cdot \mathbf{k^j}')\right] \ . \tag{4}$$

2.2 SAMoCo

The framework of SAMoCo consists of two main components, as shown in Fig. 1: (1) a pre-trained network that provides initial motion parameter estimation; (2) an instance-wise autofocusing algorithm that jointly refines motion parameters, updates coil sensitivity maps, and reconstructs motion-corrected images.

DL-based Motion Estimation To robustly infer motion priors, we propose a hybrid spatial-temporal network (Fig. 2) that explicitly encodes both multi-shot corrupted k-space and the corresponding sampling patterns, which indicates the assignment of phase encoding (PE) lines to specific shots. The k-space data are normalized and cropped to 90×90. The network first enhances k-space representations using a residual block. To achieve trajectory awareness, the sampling trajectory mask acts as a dynamic routing mechanism, guiding the network to selectively extract the PE lines corresponding to each shot and then aggregating them into a sequence of shot-wise feature vectors. The vectors are then projected into a latent space and processed by a two-layer bidirectional gated recurrent unit (Bi-GRU) with hidden size of 512, enabling flexible handling of variable-length

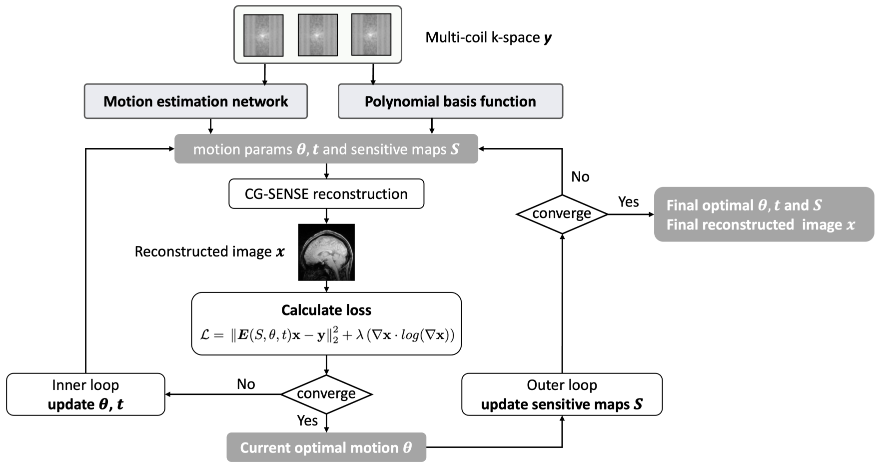

Fig. 1: Overview of SAMoCo. Motion parameters are initialized by a pre-trained network and subsequently refined jointly with sensitivity maps via autofocusing.

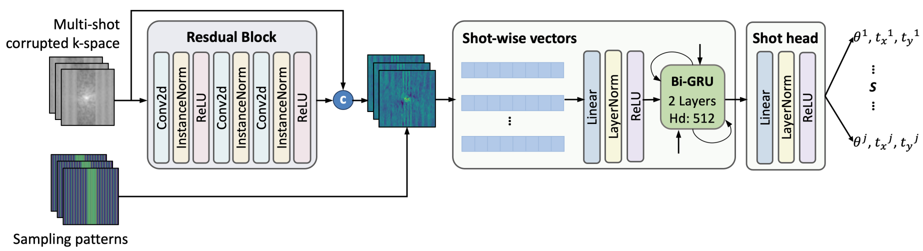

Fig. 2: Architecture of the motion estimation network, integrating residual convolutions and a Bi-GRU module to extract shot-wise motion parameters.

sequences and capturing temporal motion dependencies. A shot-wise prediction head then outputs motion parameters (θ, t_x, t_y) for each shot.

To promote sampling-agnostic motion inference, a randomized physics simulation strategy is adopted during training. K-space are selected with multiple contrasts and anatomical orientations. The rigid motion is simulated with random motion parameters and key acquisition parameters, including the number of shots, autocalibrated signal (ACS) lines, and acceleration factor (AF).

Model-based Optimization Based on the initial motion parameters inferred by the pre-trained network, we propose a physics-driven autofocusing framework to jointly refine the motion parameters and estimate the coil sensitivity maps. These maps are initialized from uncorrected images using polynomial basis functions [6, 26]. The framework consists of an inner loop and an outer loop. The outer loop updates the sensitivity maps S, while the inner loop refines the motion parameters θ and t, using adaptive moment estimation (Adam) [16] with S fixed. At each Adam iteration, conjugate gradient sensitivity encoding (CG-SENSE) [1] solver is used to reconstruct the image $\mathbf{x}$ based on the current estimates of S, θ, t. The motion parameter refinement is achieved by minimizing the following objective function, which combines data consistency with gradient entropy [19]:

$$\mathcal{L} = \|\boldsymbol{E}(S, \theta, t)\mathbf{x} - \mathbf{y}\|_2^2 + \lambda \left(\nabla \mathbf{x} \cdot log(\nabla \mathbf{x})\right) , \tag{5}$$

where $\boldsymbol{E}$ represents the motion forward operator as described in Equation 1 and ∇ represents the image intensity gradient. In the outer loop, the refined motion parameters θ, t are fixed to update S. The maps are modeled as sums of polynomial basis functions:

$$\boldsymbol{S} = \sum_c a_c \boldsymbol{B}_c \ . \tag{6}$$

The updated sensitivity maps are then fed back into the inner Adam loop for further motion refinement. This alternating optimization continues until overall convergence, yielding jointly optimized motion parameters θ, t, sensitivity maps S, and the final corrected image $\mathbf{x}$.

3 Experiments

Data for Motion Estimation There were 178 subjects per T1-, T2-, and PD-weighted contrast from the IXI (http://brain-development.org/ixi-dataset/) dataset across axial and sagittal planes. Notably, all images were acquired in a multi-shot manner with varying echo-train-lengths. The dataset was partitioned by subject into training, validation, and test sets with an 8:1:1 ratio. Corrupted k-space was simulated using random motion, with parameters independently sampled from uniform distribution $U(-3, 3)$ for each shot. The simulation employed a center-out k-space filling order with randomized acquisition parameters (shots $\in [4, 12]$, ACS $\in [10, 40]$, AF $\in [1, 3]$), resulting in a total of 267,000 slices.

Evaluation Data for Motion Correction We utilized 45 multi-coil axial slices from the fastMRI dataset [17, 27] (3 subjects $\times$ 5 slices across T1-, T2- and FLAIR-weighted) to evaluated the SAMoCo. To assess generalization, we additionally acquired 15 sagittal T2-weighted slices from three subjects on a 3T UIH scanner. All evaluation data were retrospectively corrupted with randomized motion and sampling parameters.

Implementation Details The motion estimation network was trained with a batch size of 360 and an initial learning rate (LR) of 10^{-4}, decayed by 0.1 every 50 epochs. Early stopping was triggered if loss reduction fell below 10^{-8} for 10 epochs. For the instance-wise autofocusing, coil sensitivity maps were modeled using polynomial basis functions of order 11. The hyper-parameter λ

of the objective function in Equation 5 was set to 0.01. The inner-loop Adam optimizer used an initial LR of 0.2, decayed by 0.5 after each joint outer-loop update. All models were implemented in PyTorch on RTX 4090 GPU.

Reconstruction Methods Comparison We compared our SAMoCo approach against five representative baselines: zero-filling, standard CG-SENSE, an image-domain U-Net [3] (trained on 300 fastMRI subjects), AF+ [18] (conventional autofocusing with a U-Net prior), and JSMoCo [6] (an unsupervised instance-wise framework). All methods were evaluated on the 60 motion-corrupted k-space slices from the fastMRI and in-house datasets, considering two different acceleration factors (AF=2 and AF=3).

Ablation Study To assess the contribution of each component in SAMoCo, we performed an ablation study comparing:(1) CG-SENSE reconstruction without motion correction; (2) reconstruction corrected using the initial motion parameters inferred by the pre-trained network (init corr); and (3) reconstruction corrected using final motion parameters refined by autofocusing (final corr).

4 Results

We conducted quantitative and qualitative evaluations of the different comparative methods under AF=2. As illustrated in Fig. 3, the proposed SAMoCo produced the most accurate anatomical details with minimal residual artifacts. Consistently, Table 1 demonstrates that our approach achieved the best performance across all quantitative metrics on both datasets. On fastMRI, our method attained an SSIM of 0.9721 ± 0.0093, a PSNR of 39.1100 ± 1.8554 dB, and the lowest NRMSE of 0.0185 ± 0.0041, outperforming the strongest baseline JSMoCo. Similar improvements were observed on the in-house dataset, where SSIM and PSNR reach 0.9958 ± 0.0016 and 43.5021 ± 2.3129 dB, respectively, with NRMSE reduced to 0.0110 ± 0.0033.

Further more, we extended our comparisons to a more higher acceleration (AF=3). As detailed in Table 2, the proposed method exhibited superiority over other baseline approaches. It outperformed the JSMoCo by over 0.0232 in SSIM and 3.3038 dB in PSNR on the fastMRI dataset, with corresponding improvements of 0.0237 in SSIM and 3.8635 dB in PSNR on the in-house dataset.

Fig. 4 illustrates the quantitative ablation of our proposed pipeline on the fastMRI and in-house datasets under AF=2 and AF=3. The CG-SENSE reconstruction without motion correction suffered from severe degradation. Incorporating the DL-based initial motion parameters (init corr) substantially boosted SSIM and PSNR. Autofocusing refinement (final corr) further enhanced reconstruction quality, achieving the highest SSIM and PSNR. At AF=2, the average MAE of the initial motion parameters was 0.1946 on fastMRI and 0.2753 on in-house data, which decreases to 0.0236 and 0.0324 after refinement, respectively. These consistent improvements were similarly maintained under higher acceleration (AF=3), confirming the robust correcting capability of the method.

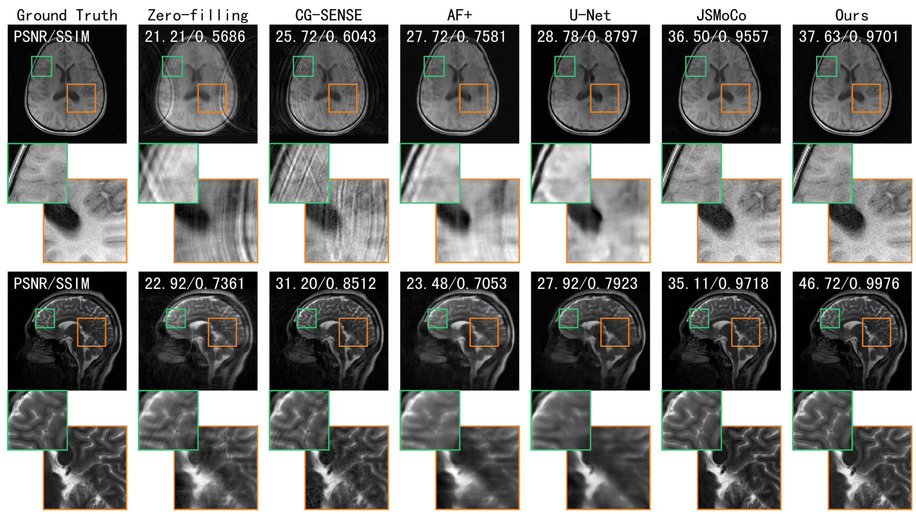

Fig. 3: Visual comparison of different motion correction methods for a corrupted data under AF=2. The first and third rows illustrate the results on fastMRI T1-weighted axial and in-house T2-weighted sagittal images, respectively.

Table 1: Quantitative comparison under AF=2.

Dataset	Methods	SSIM	PSNR	NRMSE
fastMRI	Zero-filling	0.5243±0.0865	20.5186±2.9622	33.7699±11.7640
	CG-SENSE [1]	0.6710±0.0752	24.4894±3.2635	0.0671±0.0278
	AF+ [18]	0.7558±0.0442	22.5373±3.2683	0.0901±0.0486
	U-Net [3]	0.8546±0.0399	25.0778±3.3625	0.0854±0.0346
	JSMoCo [6]	0.9521±0.0098	36.3157±2.1398	0.0226±0.0069
	Ours	**0.9721±0.0093**	**39.1100±1.8554**	**0.0185±0.0041**
in-house	Zero-filling	0.6648±0.0545	23.7284±1.7214	16.9726±3.3622
	CG-SENSE [1]	0.7454±0.0654	27.7532±1.7846	0.0433±0.0092
	AF+ [18]	0.6551±0.0644	24.1195±1.3820	0.0648±0.0112
	U-Net [3]	0.8785±0.0107	26.0819±1.6566	0.0814±0.0157
	JSMoCo [6]	0.9616±0.0070	36.8279±1.4562	0.0236±0.0036
	Ours	**0.9958±0.0016**	**43.5021±2.3129**	**0.0110±0.0033**

5 Discussion

In this study, we proposed a hybrid retrospective motion correction framework that synergistically combines DL-based initialization with physics-driven autofocusing. Ablation studies confirm the complementary roles of the two modules. The DL model provides highly accurate motion priors, and autofocusing refinement further reduces the residual MAE by over 70%.

Methodologically, the compared approaches differ substantially. U-Net operates purely in the image domain, while AF+ takes single-coil k-space as in-

Table 2: Quantitative comparison under AF=3.

Dataset	Methods	SSIM	PSNR	NRMSE
fastMRI	Zero-filling	0.5060±0.0970	19.7930±3.2596	37.1909±14.9826
	CG-SENSE [1]	0.6605±0.0810	24.1141±3.4317	0.0702±0.0300
	AF+ [18]	0.7299±0.0402	22.1495±2.5783	0.0884±0.0302
	U-Net [3]	0.8275±0.0502	23.7989±3.3780	0.0992±0.0461
	JSMoCo [6]	0.9429±0.0156	32.8771±3.3531	0.0359±0.0139
	Ours	**0.9661±0.0125**	**36.1809±1.8960**	**0.0247±0.0061**
in-house	Zero-filling	0.6084±0.0619	21.9958±2.0812	20.8506±4.4327
	CG-SENSE [1]	0.7169±0.0637	26.6545±2.0081	0.0493±0.0109
	AF+ [18]	0.5990±0.0468	21.8732±1.8315	0.0840±0.0171
	U-Net [3]	0.8475±0.0202	23.9877±1.5483	0.1023±0.0160
	JSMoCo [6]	0.9658±0.0085	35.8564±1.4795	0.0257±0.0038
	Ours	**0.9895±0.0067**	**39.7199±3.0737**	**0.0175±0.0072**

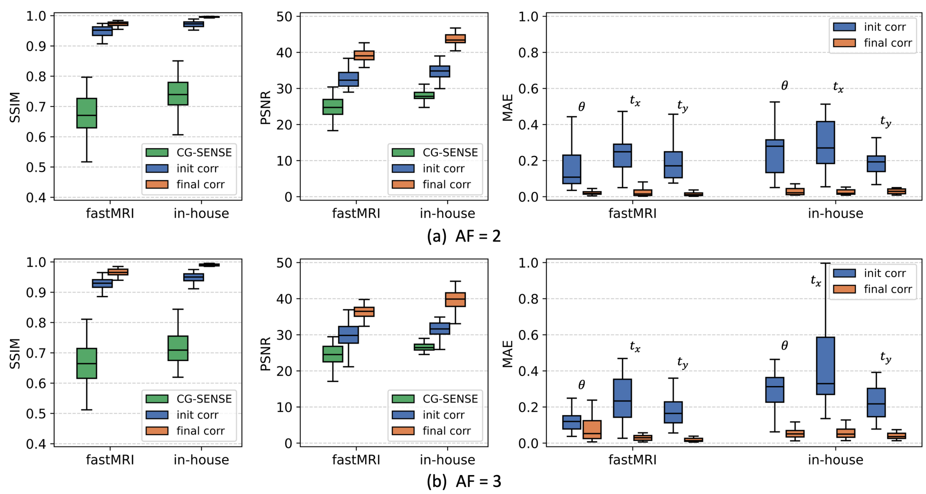

Fig. 4: Quantitative ablation analysis of SSIM, PSNR, and MAE on the fastMRI and in-house datasets under AF=2 and AF=3.

put. Standard zero-filling and CG-SENSE rely on fixed sensitivity map assumptions while JSMoCo and SAMoCo jointly update sensitivity maps. Our SAMoCo framework further improves reconstruction fidelity and outperforms the strongest baseline with SSIM/PSNR improvements of 2.1%/7.7% on fastMRI and 3.6%/18.1% on in-house data. Under the more challenging accelerate condition (AF=3), SAMoCo reliably maintains best performance, delivering consistent gains of 2.5% in SSIM and >10% in PSNR across both datasets.

Limitations The current framework is limited to 2D rigid motion and assumes motion to be negligible within each shot. Future work will extend the method to

3D non-rigid and continuous motion, as well as broader non-Cartesian sampling trajectories.

Conclusion In this work, we presented a hybrid motion correction framework that combines DL-based initialization with autofocusing optimization. The proposed synergy enables accurate motion estimation, stable convergence, and reconstruction strictly consistent with the MRI acquisition model. Comprehensive evaluations demonstrate consistent advantages over SOTA methods across datasets and acceleration factors, underscoring its potential for robust and clinically applicable motion-robust MRI reconstruction.

Acknowledgments This work received support from the National Natural Science Foundation of China (62401363), Shanghai Pujiang Program (24PJA047), and Xiaomi Young Scholar Program.

Disclosure of Interests The authors have no competing interests to declare that are relevant to the content of this article.

References

1. Aggarwal, H.K., Mani, M.P., Jacob, M.: MoDL: Model-based deep learning architecture for inverse problems. IEEE Trans. Med. Imaging **38**(2), 394–405 (2018)
2. Al-Haj Hemidi, Z., Weihsbach, C., Heinrich, M.P.: IM-MoCo: Self-supervised MRI Motion Correction Using Motion-Guided Implicit Neural Representations. In: Linguraru, M.G., Dou, Q., Feragen, A., Giannarou, S., Glocker, B., Lekadir, K., Schnabel, J.A. (eds.) MICCAI 2024, LNCS. vol. 15007, pp. 382–392. Springer, Cham (2024). `https://doi.org/https://doi.org/10.1007/978-3-031-72104-5_37`
3. Al-Masni, M.A., Lee, S., Yi, J., Kim, S., Gho, S.M., Choi, Y.H., Kim, D.H.: Stacked U-Nets with self-assisted priors towards robust correction of rigid motion artifact in brain MRI. Neuroimage **259**, 119411 (2022)
4. Atkinson, D., Hill, D.L., Stoyle, P.N., Summers, P.E., Keevil, S.F.: Automatic correction of motion artifacts in magnetic resonance images using an entropy focus criterion. IEEE Trans. Med. Imaging **16**(6), 903–910 (1997)
5. Chen, L., Balter, J.M., Shen, L., Park, J.J.: Single-Spoke Motion-Compensated Dynamic 3D MRI Reconstruction via Neural Representation. In: Gee, J.C., Alexander, D.C., Hong, J., Iglesias, J.E., Sudre, C.H., Venkataraman, A., Golland, P., Kim, J.H., Park, J. (eds.) MICCAI 2025, LNCS. vol. 15972, pp. 513–522. Springer, Cham (2025). `https://doi.org/https://doi.org/10.1007/978-3-032-05169-1_38`
6. Chen, L., Tian, X., Wu, J., Feng, R., Lao, G., Zhang, Y., Liao, H., Wei, H.: Joint coil sensitivity and motion correction in parallel MRI with a self-calibrating score-based diffusion model. Med. Image Anal. **102**, 103502 (2025)
7. Chen, Z., Pawar, K., Ekanayake, M., Pain, C., Zhong, S., Egan, G.F.: Deep learning for image enhancement and correction in magnetic resonance imaging—state-of-the-art and challenges. J. Digit. Imaging **36**(1), 204–230 (2023)
8. Cui, L., Song, Y., Wang, Y., Wang, R., Wu, D., Xie, H., Li, J., Yang, G.: Motion artifact reduction for magnetic resonance imaging with deep learning and k-space analysis. PLoS One **18**(1), e0278668 (2023)

9. Dabrowski, O., Falcone, J.L., Klauser, A., Songeon, J., Kocher, M., Chopard, B., Lazeyras, F., Courvoisier, S.: SISMIK for brain MRI: Deep-learning-based motion estimation and model-based motion correction in k-space. IEEE Trans. Med. Imaging (2024)
10. Eichhorn, H., Hammernik, K., Spieker, V., Epp, S.M., Rueckert, D., Preibisch, C., Schnabel, J.A.: Physics-Aware Motion Simulation For T2*-Weighted Brain MRI. In: Wolterink, J.M., Svoboda, D., Zhao, C., Fernandez, V. (eds.) SASHIMI 2023, LNCS. vol. 14288, pp. 42–52. Springer, Cham (2023). https://doi.org/https://doi.org/10.1007/978-3-031-44689-4_5
11. Fessler, J.A., Sutton, B.P.: Nonuniform fast Fourier transforms using min-max interpolation. IEEE Trans. Signal Process. **51**(2), 560–574 (2003)
12. Godenschweger, F., Kägebein, U., Stucht, D., Yarach, U., Sciarra, A., Yakupov, R., Lüsebrink, F., Schulze, P., Speck, O.: Motion correction in MRI of the brain. Phys. Med. Biol. **61**(5), R32–R56 (2016)
13. Haskell, M.W., Cauley, S.F., Wald, L.L.: TArgeted Motion Estimation and Reduction (TAMER): data consistency based motion mitigation for MRI using a reduced model joint optimization. IEEE Trans. Med. Imaging **37**(5), 1253–1265 (2018)
14. Hossbach, J., Splitthoff, D.N., Cauley, S., Clifford, B., Polak, D., Lo, W.C., Meyer, H., Maier, A.: Deep learning-based motion quantification from k-space for fast model-based magnetic resonance imaging motion correction. Med. Phys. **50**(4), 2148–2161 (2023)
15. Iyer, S., Ong, F., Setsompop, K., Doneva, M., Lustig, M.: SURE-based automatic parameter selection for ESPIRiT calibration. Magn. Reson. Med. **84**(6), 3423–3437 (2020)
16. Kingma, D.P., Ba, J.: Adam: A method for stochastic optimization. arXiv preprint arXiv:1412.6980 (2014)
17. Knoll, F., Zbontar, J., Sriram, A., Muckley, M.J., Bruno, M., Defazio, A., Parente, M., Geras, K.J., Katsnelson, J., Chandarana, H., et al.: fastMRI: A publicly available raw k-space and DICOM dataset of knee images for accelerated MR image reconstruction using machine learning. Radiology **2**(1), e190007 (2020)
18. Kuzmina, E., Razumov, A., Rogov, O.Y., Adalsteinsson, E., White, J., Dylov, D.V.: Autofocusing+: Noise-Resilient Motion Correction in Magnetic Resonance Imaging. In: Wang, L., Dou, Q., Fletcher, P.T., Speidel, S., Li, S. (eds.) MICCAI 2022, LNCS. vol. 13436, pp. 365–375. Springer, Cham (2022). https://doi.org/https://doi.org/10.1007/978-3-031-16446-0_35
19. McGee, K.P., Manduca, A., Felmlee, J.P., Riederer, S.J., Ehman, R.L.: Image metric-based correction (autocorrection) of motion effects: analysis of image metrics. J. Magn. Reson. Imaging **11**(2), 174–181 (2000)
20. Pan, J., Rueckert, D., Küstner, T., Hammernik, K.: Learning-Based and Unrolled Motion-Compensated Reconstruction for Cardiac MR CINE Imaging. In: Wang, L., Dou, Q., Fletcher, P.T., Speidel, S., Li, S. (eds.) MICCAI 2022, LNCS. vol. 13436, pp. 686–696. Springer, Cham (2022). https://doi.org/https://doi.org/10.1007/978-3-031-16446-0_65
21. Qiao, X., Li, W., Xiao, B., Huang, Y., Yang, L.: Stacking u-nets in u-shape: Redesigning the information flow in model-based networks for mri reconstruction. In: ICASSP 2025-2025 IEEE International Conference on Acoustics, Speech and Signal Processing (ICASSP). pp. 1–5. IEEE (2025)
22. Spieker, V., Eichhorn, H., Hammernik, K., Rueckert, D., Preibisch, C., Karampinos, D.C., Schnabel, J.A.: Deep learning for retrospective motion correction in MRI: a comprehensive review. IEEE Trans. Med. Imaging **43**(2), 846–859 (2023)

23. Sun, H., Li, Y., Li, Z., Yang, R., Xu, Z., Dou, J., Qi, H., Chen, H.: Fourier convolution block with global receptive field for MRI reconstruction. Med. Image Anal. **99**, 103349 (2025)
24. Wang, F., Tamir, J.I.: Non-rigid motion correction for mri reconstruction via coarse-to-fine diffusion models. In: 2025 IEEE International Conference on Image Processing (ICIP). pp. 1061–1066. IEEE (2025)
25. Wang, J., Yang, H., Yang, Y., Sun, J.: MRI Motion Artifact Correction via Frequency-Assisted Artifact Disentanglement and Confidence-Guided Knowledge Distillation. In: Gee, J.C., Alexander, D.C., Hong, J., Iglesias, J.E., Sudre, C.H., Venkataraman, A., Golland, P., Kim, J.H., Park, J. (eds.) MICCAI 2025, LNCS. vol. 15972, pp. 392–401. Springer, Cham (2025). `https://doi.org/https://doi.org/10.1007/978-3-032-05169-1_38`
26. Ying, L., Sheng, J.: Joint image reconstruction and sensitivity estimation in SENSE (JSENSE). Magn. Reson. Med. **57**(6), 1196–1202 (2007)
27. Zbontar, J., Knoll, F., Sriram, A., Murrell, T., Huang, Z., Muckley, M.J., Defazio, A., Stern, R., Johnson, P., Bruno, M., et al.: fastMRI: An open dataset and benchmarks for accelerated MRI. arXiv preprint arXiv:1811.08839 (2018)
28. Zoroofi, R.A., Sato, Y., Tamura, S., Naito, H.: MRI artifact cancellation due to rigid motion in the imaging plane. IEEE Trans. Med. Imaging **15**(6), 768–784 (1996)